TITLE: Machine Learning Based Modelling of Human and Insect Olfaction Screens Millions of compounds to Identify Pleasant Smelling Insect Repellents

AUTHORS: Joel Kowalewski[1], Sean M. Boyle[2], Ryan Arvidson[2], Jadrian Ejercito[2], and Anandasankar Ray[1,2]

AFFILIATION:

[1]Interdepartmental Neuroscience Program

[2]Department of Molecular, Cell and Systems Biology

University of California, Riverside, CA 92521, USA

CORRESPONDING AUTHOR: Anandasankar Ray

Department of Molecular Cell and Systems Biology, University of California Riverside, 3401 Watkins Drive, Riverside, CA 92521, USA, Phone:+1(951) 827-5998, Email: anand.ray@ucr.edu

Abstract

The rational discovery of behaviorally active odorants is impeded by limited information on how the olfactory system generates percept or valence for a volatile chemical. In previous studies, we showed that chemical informatics could be used to predict ligands for a large repertoire of odorant receptors in *Drosophila* (Boyle et al., 2013). However, it remained difficult to predict behavioral valence of volatiles since the activities of a large ensembles of odor receptors encode odor information, and little is known about the complex information processing circuitry. This is a systems-level challenge well-suited for Machine-learning approaches which we have used to model olfaction in two organisms with completely unrelated olfactory receptor proteins: humans (~400 GPCRs) and insects (~100 ion-channels). We use chemical structure-based Machine Learning models for prediction of valence in insects and for 146 human odor characters. Using these predictive models, we evaluate a vast chemical space of >10 million compounds *in silico.* Validations of human and insect behaviors yield very high success rates. The discovery of desirable fragrances for humans that are highly repulsive to insects offers a powerful integrated approach to discover new insect repellents.

Introduction

Animals can detect volatile molecules in their environment using specialized protein receptors in their olfactory organs. Mammalian odorant receptors were discovered in 1991 and are G-protein coupled receptors (GPCRs) numbering >400 in humans (Buck L and Axel, 1991). Several years later starting in 1999 three families of distinct insect odorant receptors were discovered from the *Drosophila* genome which are ligand-gated ion channels and number ~100 (Clyne et al., 1999, 2000). Over the subsequent 20-30 years, studies in mice and insects focusing on odor detection, odorant receptors, odorant receptor neurons, and higher-level circuitry, have revealed important principles. A single volatile is usually detected

41 by a combination of receptors, and the activity from the neural circuit processing the information is
42 extremely complex. Previously, we successfully developed a chemical informatics approach to discover
43 ligands for a large number of odorant receptors in *Drosophila* (Boyle et al., 2013). However, the
44 mechanisms connecting olfactory perception (e.g., rose, lemon, pleasant, unpleasant, etc.) to olfactory
45 receptor activity are incompletely understood and it is therefore challenging to predict behavior from
46 odorant receptor activity alone. There is also often a lack of correspondence between simple, 2D
47 representations of odorants and their perceptual descriptions, and the molecular-cellular organization of
48 the olfactory system lacks a simple discernible coding strategy that enables predictions, unlike auditory
49 or visual processing (Buck L and Axel, 1991; Grabe & Sachse, 2018; P Mombaerts, 1999; Peter Mombaerts,
50 2001; Sachse & Beshel, 2016; Vassar et al., 1993).

51 Yet Machine Learning algorithms have shown promise in accurately predicting human odor
52 perception (Keller et al., 2017; Kowalewski et al., 2021; Kowalewski & Ray, 2020b; Lee et al., 2023;
53 Sanchez-Lengeling et al., 2019). Recently, we have shown that the volatile structure-to-percept prediction
54 can be improved by using the activities of a small number of human odorant receptors and applying
55 machine learning algorithms to identify highly predictive combinations (Kowalewski & Ray, 2020b). In
56 insects, we have limited success modeling the behavioral valence of volatiles from olfactory receptor
57 neuron activity in the fruit fly, *Drosophila melanogaster*. Since receptor activity depends on chemical
58 structure, this suggests machine learning algorithms can potentially detect a consistent physicochemical
59 basis for simple behavioral or complex perceptual responses (Kowalewski & Ray, 2020b; MacWilliam et
60 al., 2018).

61 To test whether Machine learning based modeling can lead to identification of strong behaviorally
62 active volatiles, we selected a challenge that has a very high potential for easing human suffering and yet
63 had little innovation: pleasant smelling fragrances that are also repulsive to harmful insects that transmit
64 diseases to humans or cause agricultural loss. Annually, mosquitos account for ~500,000-700,000 deaths

65 and a billion infections due to vector-borne illnesses like malaria, Dengue, Yellow Fever. Insects also
66 destroy ~30% of the global agricultural produce causing additional suffering. Insects are currently
67 managed through widespread application of insecticides, but mutations are emerging that confer
68 insecticide resistance and affect insect olfactory responses in both human disease vectors and plant pests
69 (Deletre et al., 2019; Duneau et al., 2018).

70 The most widely used topical repellent for mosquitoes is DEET (N,N-Diethyl-m-toluamide), a
71 chemical with undesirable chemical and cosmetic properties. DEET (N,N-Diethyl-m-toluamide) was
72 discovered >75 years ago through empirical testing. It is not widely used outside the developed world,
73 where vector borne diseases are present globally, and are also use restrictions due to its strong solvent
74 properties, even dissolving plastics and nylons. Recent studies have also raised human health concerns ,
75 as the chemical interferes with inhibitory neurotransmission in mammals via $GABA_A$ and Glycine receptors
76 (Grant & Hall, 2019). Unfortunately, not enough is understood about the odorant receptors for aversion
77 in mosquitoes as a result there has been limited innovation in the search for repellents even a quarter
78 century after discovery of insect odorant receptors. The last repellent registered by the US EPA for
79 commercial use was Picaridin, over 20 years ago.

80 Volatile compounds that have pleasant fragrances are desired by humans in cosmetics and are
81 therefore excellent candidates for novel mosquito repellents. In order to identify fragrances that would
82 be aversive to insects, we assumed machine learning (ML) could be used to identify structural features
83 enriched among repellents and then detect these features within any arbitrary, large chemical space
84 (Maldonado et al., 2006). We trained a support vector machine (SVM) on a comprehensive set of
85 chemicals with known repellency from literature and identified predictive physicochemical features. In
86 parallel, we adapted a collection of recently developed ML models to predict 146 different human odor
87 percepts, helping us organize the candidate repellents by their potential fragrances (Kowalewski et al.,
88 2021; Kowalewski & Ray, 2020b). We then validated the accuracy of behavioral predictions for insects and

89 humans by randomly testing 50 predicted chemicals for repellency in mosquitoes and odor perception in
90 humans. The validation success was >75% in each assay, repellent and perceptual, with ~95% of the
91 chemicals tested for repellency in round 1 showing aversion, which left ~5% as neutral or slightly attractive
92 to mosquitoes. Collectively, this suggests a strong physicochemical basis for odor valence and percept in
93 insects and humans. In addition, we also built *in silico* toxicity models, filtering the compounds across
94 multiple parameters for human use. A small number of the fragrances were tested on evolutionarily
95 distinct insects, finding that they are repellent to mosquitoes and the fruit fly, *Drosophila*.

96 Tens of millions of dollars and several years may be required for identification and adequate
97 human-safety analysis for registration of new repellent chemicals by the EPA (Gupta & Bhattacharjee,
98 2006). Machine learning approaches for modeling toxicity as well as other physical and cosmetic attributes
99 are steadily advancing, suggesting it is possible to accelerate this search and significantly reduce costs.
100 Accordingly, we included additional computational filters to select predicted repellents such as predicted
101 fragrant odor perceptual qualities. Because fragrant molecules that are also insect repellents may be rare
102 to find, we applied this approach to a large library (>10 million) of purchasable chemicals from the ZINC
103 15 database. These efforts represent a dramatic expansion of the insect repellent chemical space and
104 provides a theory-based high-throughput method to drive rational discovery of novel insect repellents.

105

106 **Results**

107 **Machine learning can learn to predict aversive valence in insects from chemical structure**

108 To predict insect behavior, we developed a novel chemical informatics approach using Machine Learning
109 (ML). We assembled a training set of volatile chemicals known in the literature to have a negative
110 behavioral valence including eucalyptol, linalool, geraniol, citronella, alpha-thujone, beta-thujone (Kline
111 et al., 2003; Klocke et al., 1987; Syed & Leal, 2008), DEET, picaridin, 34 N-acyl piperidines that are

112 structurally related to picaridin (Katritzky et al., 2008) and structurally diverse odorants from fruits and
113 food sources that are not expected to elicit aversion (Carey et al., 2010; Hallem & Carlson, 2006). We
114 generated energy-minimized 3D structures for each and calculated 3,242 physicochemical features for
115 201 training chemicals. From it we identified 18 features that were highly correlated with aversive valence
116 (correlation of 0.912). We then fit a support vector machine (SVM) with these features to learn to predict
117 the repellency of test chemicals (Figure 1).

118 The trained model successfully predicted the valence of the test chemicals (avg AUC = 0.994),
119 indicating that it could distinguish volatiles with aversive valence from non-repellents (Figure 1).
120 Evaluation of the predictive chemical features indicated six membered rings, carbon-nitrogen distances,
121 tertiary amides, and the positioning of oxygen atoms in the molecule are associated with repellency
122 (Figure 1).

123 We subsequently used this repellency model to evaluate a >440,000 small molecules assembled
124 from databases which includes ~3,000 chemicals from natural sources like plants, insects, vertebrates,
125 and compounds that are in food, beverages, and cosmetics. The top 500 predicted compounds (top ~0.1%
126 of hits) represent a structurally diverse group of chemicals, with some showing similarities to volatiles in
127 the training set (Figure 1). Several naturally occurring compounds were also in the list of precited
128 repellents. Since the ML model successfully classified known repellents versus non-repellents, we next
129 experimentally tested the candidate repellents.

130 **Machine learning can prioritize candidate repellents by modeling their odor qualities to humans**

131 Importantly, repellents must meet many physical and cosmetic demands for human use. However,
132 evaluating the scent characteristics of candidate repellents with human subjects is a laborious, expensive,
133 and time-consuming task. In order to create a method to bypass this bottleneck, we adapted our recent
134 perceptual modeling approach involving the prediction of 146 odor perceptual descriptors from chemical

135 structure; example perceptual descriptors include “fruity other than citrus”, “lemon”, “orange”,
136 “cinnamon”, “perfumery” and unpleasant ones such as “sickening”, “rancid”, “animal”, and “dirty linen”
137 to name a few (Kowalewski et al., 2021; Kowalewski & Ray, 2020b). The models were trained with data
138 from prior human behavior studies in which participants evaluated ~150 odorants and mixtures according
139 to the 146 descriptors. The development of the methods and validation of the models were rigorously
140 evaluated in the previous publications (Kowalewski et al., 2021; Kowalewski & Ray, 2020b). Using these
141 models, we predicted odor descriptors for the candidate insect repellents that were discovered using the
142 model described in Figure 1. The compounds had a wide variety of predicted odor characteristics covering
143 both pleasant and unpleasant fragrance profiles. Together with the insect valence predictions, this gives
144 us the foundations for selecting desirable fragrances that can protect humans and plants from pests.

145 **Validation of computational behavioral predictions of human smell and insect aversion**

146 To validate the behavioral predictions of scent or repellency, on humans and insects, respectively,
147 we selected 44 compounds based on their availability and affordability. First, we compared them to
148 reports from human testing of smell properties. While odor qualities remain poorly characterized, 37 of
149 the 44 tested had odor and taste annotation in a sensorial databases at the The Good Scents Company.
150 We could then rigorously evaluate the accuracy of the trained perceptual models by ROC analysis. The
151 perceptual models predicted the observed descriptors for most volatiles with a high success rate (Avg.
152 AUC = 0.77) (Figure 2A,B). Interestingly, many chemicals in the predicted repellents have pleasant odor
153 characteristics, including highly desirable ones such as fruity, floral or perfume-like, such as seen in the
154 word cloud of enriched predicted characters for the predicted insect repellents (Figure 2C).

155 We next tested the compounds against *Aedes aegypti* mosquitoes. We developed a high
156 throughput assay utilizing the innate attraction of the female mosquitoes to a heat block approximating
157 human skin temperature (37 °C) covered with a filter paper (Figure 3A). Each of the test compounds were

158 individually evaluated by applying on the filter paper (3% in acetone) and counting the numbers of
159 mosquitoes landing on the surface with solvent control before and after applying the compound. A
160 repellency index indicated that most of the predicted compounds (~90%) showed >50% repellency to
161 female *A. aegypti* mosquitoes (Figure 3B). These results suggest that the machine learning (ML) algorithm
162 was capable of predicting a chemical's perceptual qualities for humans and its valence for insects. This set
163 of chemicals represents a very large increase in new insect repellents, comprising diverse chemical
164 structures and smell characteristics that are desirable for human use. In a separate study we had tested
165 a few of these repellents using a human arm-in-glove behavioral assay and observed strong repellency
166 (Boyle et al., 2016), suggesting that the newly discovered compounds are likely to exhibit similar effects.

167 Since we do not know the molecular receptor targets for these diverse repellents, and different
168 insect species have both highly diverse and conserved olfactory receptors, we cannot tell *a priori* whether
169 the repellency is narrowly effective in mosquitoes or conserved across diverse insects. To determine
170 broad-spectrum aversive valence among insects, we tested another distantly related dipteran, *Drosophila*
171 *melanogaster*, which is >250 MY apart evolutionarily. All of the predicted compounds displayed
172 concentration-dependent aversive valence to *Drosophila* in a trap-based 2-choice assay (Reeder et al.,
173 2009; Syed et al., 2011). Most of the tested compounds showed strong repellency (Figure 3C). The
174 simplest interpretation is that the machine learning algorithm was able to identify chemical features that
175 predict negative valence across multiple species of dipteran insects.

176 **Repellents show calcium mobilization in mammalian cells**

177 An alternative approach to identifying insect repellents would be to computationally model a known
178 cellular or molecular activity relevant to repellency. Interestingly, one of the aversive compounds used in
179 the repellency training set is the commercial repellent DEET, had previously been seen to cause calcium
180 mobilization in human HEK293 cells at high concentrations (Dennis et al., 2018). In order to further

181 evaluate if such Ca^{2+} mobilization is a common feature for repellency, we performed additional
182 experiments.

183 When HEK293 cells were exposed to DEET, a dose-dependent calcium transient was observed,
184 with an EC50 of 56.6 mM (~1% vol/vol), below the concentrations used on skin applied formulations (7-
185 98% vol/vol) of which up to 60% is absorbed into the skin (Schoenig et al., 1996; Selim et al., 1995). (Figure
186 4A). Additional cell lines from different organisms were tested, including an insect S2 cell line, and all of
187 them were sensitive to DEET at similar EC50s (Figure 4A). The DEET-induced calcium transients were
188 similar in magnitude to the positive control, a 100 µM ATP induced signal (e.g., GPCR mediated) (Figure
189 4B). To assess the source of DEET induced calcium flux, cells were depleted of intercellular calcium with
190 treatment with thapsigargin (a SERCA antagonist) 10 minutes before the assay. These calcium-depleted
191 cells did not show increased Ca transients when treated with DEET. This indicates that DEET is likely
192 inducing release from intercellular calcium stores, in a dose-dependent manner (Figure 4C). Interestingly,
193 two additional commercially used repellents, picaridin and diethyl benzamide (a structural analog of
194 DEET), also evoked a strong intracellular Ca^{2+} signal (Figure 4D). Because these three compounds were
195 part of the training data to build our machine learning insect repellent models, we tested whether the
196 newly identified aversive fragrances also showed similar activity. We tested a sampling of the verified
197 aversive fragrances, and a few traditionally known repellents, at two concentrations (5% and 0.5%) in the
198 HEK293 cell line and found that there were indeed some that showed Ca^{2+} release (Figure 4E). However,
199 there appeared to be no correlation between the repellency index and the Ca^{2+} activation of the fragrant
200 repellents (R^2=0.0093), suggesting that this conserved effect is unlikely to contribute to aversive behavior.

201 Nevertheless, the data provided an opportunity to develop a better understanding of the
202 physicochemical basis of the Ca^{2+} mobilization seen *in vitro* and we trained machine learning models to
203 predict the calcium activity (Figure S1A). Upon analyses, the top chemical features for predicting the
204 calcium activity were different from the features selected by the model to predict repellency. This too

205 suggest that while there is a structural basis for basis for calcium activity which does not overlap with
206 shared features for detection as a repellent. The features fell into 3 broad categories including 2D
207 autocorrelation, RDF, and 3D MoRSE features. Autocorrelations are distance-based metrics, with the 2D
208 autocorrelation referring to the number of bonds between a pair of atoms in the molecule, while radial
209 distribution function (RDF) features encode dependencies between atoms that give rise to molecules'
210 characteristic infrared spectra (Hemmer et al., 1999). The 3D MoRSE features are based on theoretical
211 electron diffraction patterns and are therefore sensitive to differences in 3D geometries (Devinyak et al.,
212 2014). In previous work, these features have been shown to be predictive of ligand bonding and biological
213 activity (Beglari et al., 2020; Cheng et al., 2010; González et al., 2006).

214 Evaluation of models trained with these features on test data showed a high correlation between
215 the predicted and observed Ca^{2+} activities (Figure S1). Using another approach, where we classified the
216 chemicals as broadly falling into one of two categories (high versus low activity), the predictions were also
217 accurate, further emphasizing that the Ca^{2+} signal does indeed have a strong physicochemical basis.
218 Collectively, this suggests the unique 3D shape, rather than generic, possibly indiscriminate information,
219 underlies the observed Ca^{2+} activity, supporting our contention that the activity may be a persistent off
220 target effect among certain chemical repellents and should therefore be further investigated. While the
221 physiological consequences of this effect have not been studied, we incorporated this activity as a
222 parameter into our machine learning pipeline, allowing us to further triage repellents for future use by
223 low estimated Ca^{2+} activity, in addition to other desirable characteristics for human or animal use.

224 **Mining massive commercially available chemical spaces for novel insect repellents**

225 The size and diversity of the chemical library we initially screened (~0.45M) is in the range of high-
226 throughput wet lab screening that pesticide discovery companies can undertake. The Machine learning
227 approach allows us to screen far more without the limitations of cost of synthesis and screening time. To

228 demonstrate the massive throughput capacity of this approach, we increased our search space to >10
229 million commercially available chemicals (from the ZINC 15 database), canvasing far more structural
230 diversity than the ~450,000 chemicals we previously screened. We built a new training set including the
231 chemical repellents we experimentally verified, more than doubling the number of the actives while
232 adding greater structural diversity. The top features fell mostly into 2D and 3D autocorrelations and 3D
233 MoRSE categories, suggesting that certain types of features became increasingly important following the
234 addition of more repellent activities. Notably, some features changed from this vastly improved training
235 set; that is, moving away from simple features that account for amides, or more generally, chemical bonds
236 including nitrogen (N). This possibly reflects an initial bias toward DEET, an amide, that was resolved when
237 including more complex feature selection methods and increasing the size and diversity of the training
238 set.

239 There was a strong correlation between the predicted and observed repellency when validating
240 these updated models on test data (R = 0.73). Then, by applying the filters that we progressively
241 incorporated into the pipeline, and described throughout (e.g., insect valence, odor perceptual qualities,
242 and intracellular calcium release), we identified a set of candidates still numbering in the hundreds. We
243 next predicted the acute oral mammalian toxicity (Rat) using a computational model from our earlier work
244 (Kowalewski & Ray, 2020a) and eliminated all compounds falling into EPA Tox categories I and II. The top
245 predictions contain many aminobenzoates comprised of benzene, amino, and ester groups. Some
246 chemicals notably differ in that they resemble amide repellents like diethyltoluamide (DEET) (Figure 5A).
247 The top hits were predicted to have a variety of different human odor characters, many of which are
248 perceptually pleasant or are useful in agriculture (Figure 5B). This approach accelerates the identification
249 of novel, fragrance-based, broad spectrum insect repellents.

250 **Discussion**

251 Here, we have developed a comprehensive machine learning pipeline to screen small or large
252 chemical spaces for suitable alternatives and verified numerous predicted chemicals for repellency in
253 various behavioral assays and across species, indicating the effectiveness of the pipeline. The rapid
254 identification of fragrances that have excellent behavioral activity, pleasant smell and safety greatly
255 improves the likelihood of regulatory approval and potential for use.

256 Interestingly, we identified a strong intracellular Ca^{2+} signal in response to DEET and picaridin as
257 well as some anthranilates. While the mechanism remains unclear, it has been previously observed in
258 cultured cell lines after DEET exposure (Dennis et al., 2018; Swale et al., 2014). One possibility proposed
259 in the literature is that the elevated intracellular Ca^{2+} is due to activation of octopamine receptors.
260 Octopamine plays a modulatory role, with targets including OctαR and OctαβR in insects and TAAR1 in
261 mammals (Kleinau et al., 2011; Swale et al., 2014), and while this could explain the many complex
262 physiological responses that have reported in the DEET literature (Briassoulis, 2001; Clem et al., 1993;
263 Corbel et al., 2009; Tavares et al., 2019), an unknown but conserved receptor subtype is still possible.
264 Additional research will be needed to determine whether this phenomenon is important for off-target
265 mammalian toxicity. In either case, the model we developed to predict the Ca^{2+} mobilization may help
266 isolate a set of key physicochemical features, enabling identification of compounds that have this effect.
267 However, since the calcium activity does not explain the repellency, additional electrophysiological and
268 genetic experiments are needed to further clarify the mechanism of action.

269 Although many repellents have been studied, DEET remains the most widely used commercially
270 available chemical repellent. Yet research continues to emerge about off-target toxicities in humans who
271 are repeatedly exposed to DEET; specifically, accounts suggest adverse skin reactions and activities in
272 human or broadly mammalian nervous systems (Briassoulis, 2001; Grant & Hall, 2019; Osimitz et al.,
273 2010). This study demonstrates the successful development and application of a machine learning
274 pipeline that accelerates research into insect repellency and its physicochemical basis. The methods and

275 data presented provide a high-throughput and rational way to identify additional novel repellent
276 chemicals. Here, we emphasized screening candidate chemicals that are most likely to fit multiple
277 requirements (smell and repellency) rather than simply repellency. As these requirements steadily
278 increase, it is obvious that massive, unexplored chemical spaces offer the most promising leads. By
279 predicting and filtering 10+ million purchasable chemicals according to their desirability for human use,
280 we further illustrate an essential role for computational approaches (e.g., machine learning) in future
281 repellency studies, accelerating the discovery of safe, ecologically friendly, and effective repellent
282 chemicals.

Material and Methods

Behavior testing

Repellency Assay in Drosophila

Repellency was tested using a *Drosophila melanogaster* Canton S strain (RRID:BDSC_1), backcrossed >5 generations to w1118 (RRID:BDSC_3605) strain in 2-choice trap assay. All chemicals were purchased at highest purity from Sigma Aldrich (RRID:SCR_008988), TCI, Alfa Aesar, Penta, Parachem, Bedoukian, and Molbase. A chamber was built from DRAM vials, with four air holes made in the plastic lid and the bottom of chamber is coated with 5 ml of 1% agarose to maintain moisture. Traps are made from 1.5 ml Natural Microcentrifuge tubes with bottom 3 mm cut to form an opening and a 1000 ul blue graduated pipette tip catalogue number 1111-2023. To create a plastic funnel, a pipette tip was cut on both ends; cut to 1.0 cm from tip end to expand the opening of the funnel and then cut on the other end of plastic to create a final height of 2.5 cm for funnel. A BioRad PCR 0.2 ml Tube cap was cut from the strip and was inserted into the lid of microcentrifuge tube. Test odor (35 ul) was placed in the PCR tube cap and lure (90 ul) was placed in outer ring between the PCR cap and the microcentrifuge cap. In the dark, 4–7-day old, starved flies (10 males, 10 females) were released per trap and followed for 2 days. Counts were taken manually, and the Preference Index (PI) was computed using the formula below.

$$Preference\ Index\ (PI) = \frac{(\#\ flies\ in\ treated\ trap) - (\#\ flies\ in\ control\ trap)}{(\#\ files\ in\ test\ trap) + (\#\ flies\ in\ control\ trap)}$$

Repellency Assay in Mosquitoes

A non-contact heat attraction assay was performed by simultaneously offering mated female *Aedes aegypti* mosquitoes that were ~4-10 days old, a test chemical on a filter paper coupled with an attractive heat source. Heat for the assay was provided by a Hot hands® Hand warmers HH2 (Heat Max, Dalton, GA) which was activated by shaking in gloved hands. Temperature (~37°C) was verified using IR thermometers.

305 The hand warmer was fitted snugly into a 100 mm x 15 mm petri dish base and covered with 15 cm x 15
306 cm piece of polyester net secured round the petri dish by a pair or 8-inch plastic cable ties (Gardner
307 Bender, Milwaukee, WI). The petri dish with hand warmer was covered with a larger 150 mm X 15 mm
308 petri dish with a 10 cm x 7.5 cm rectangular window cut out. This netted window aligned with the hand
309 warmers exposing a heated surface.

310 A polyester net (measuring 9 cm x 8 cm) was treated with 500 µl of either acetone (solvent) or 3%
311 (v/v or w/v) test chemical and allowed to air dry for 30 minutes to evaporate solvent. The test compound
312 (~0.2mg/cm^2) treated net was secured by stretching between a frame made using two 10 cm x 7.5 cm
313 flexible magnetic frames with 7.5 cm x 6.2 cm cut out windows. This dose is 88% lower than the amount
314 recommended in the WHO, WHOPES "Guidelines for Efficacy Testing of Mosquito Repellents for Human
315 Skin" recommended dose (~1.67mg/cm^2) actives. Three more flexible magnets were added on top as
316 spacers from the heat source. The net-magnet assembly was placed directly over the 10 cm x 7.5 cm cut
317 out openings of the larger 150 mm X 15 mm petri dishes holding the heat pads. The stimulus was placed
318 on the top net of the frames. Temperature was monitored by a laser Infra-red thermometer and assay
319 started at 37°C. A puff of 5% CO_2 was blown into the cage to behaviorally activate the mosquitoes and
320 initiate the assay. A webcam timelapse is used to record mosquitoes landing on the net for automated
321 counting offline using ImageJ (RRID:SCR_003070). A custom Macro is used in ImageJ (RRID:SCR_003070)
322 to count the mosquitoes in the selected area (the net) across the timepoints. The counts from each frame
323 are automatically tabulated.

324 **Macro:**

```
325 run("8-bit");
326 setAutoThreshold("Default");
327 //run("Threshold...");
```

```
setThreshold(0, 80);
run("Analyze Particles...", "size=2-70 show=[Overlay Outlines] clear summarize stack");
dir = getDirectory("image");
name = getTitle;
index = lastIndexOf(name, ".");
if (index!=-1) name = substring(name, 0, index);
name = name + ".csv";
selectWindow("Summary of "+getTitle);
saveAs("Measurements", dir+name);
```

Since this is a 1-choice assay, for each cage and compound, a solvent alone control is done before and after the test material, with at least 20 minutes between the trials. Any significant changes in behavior between the control solvent should indicate if mosquito behavior is acceptable.

Repellency coefficient = (mean cumulative number of mosquitoes on solvent treated control netting – mean cumulative number of mosquitoes on treated netting)/ mean cumulative number mosquitoes attracted to solvent treated control netting. Cumulative number of mosquitoes on the window of treatment are counted for at time points 2,3,4,5 min. Each compound has 2-23 trials, ~40 mosquitoes per trial.

In vitro assay of Ca^{2+} mobilization

All mammalian cell lines were maintained at 37 C, 5% CO2, and 99 percent relative humidity. Insect Schneider 2 (S2) Cells (RRID: CVCL_Z232**)** were maintained at 26 C and 99% relative humidity. HEK293T (ATCC, RRID:CVCL_0063), CHOk1 (RRID: CVCL_E8IB) and NG108-15 (RRID: CVCL_0464) were grown in

349 DMEM media (Gibco), supplemented with 10% FBS (Gibco), and antibiotic-antimycotic supplement
350 (Gibco). S2 cells (RRID: CVCL_Z232**)** were cultured in Shields and Sang M3 Insect Medium (Sigma),
351 supplemented with Insect Medium Supplement (Sigma). Cells were transfected with the luminescent
352 calcium reporter aequorin 24 hours before experiment with X-tremeGENE 9 transfection reagent, in the
353 case of HEK293T (and CHOK1, and X-tremeGENE HP, in the case of NG108 and S2 cells. Transfected cells
354 were harvested with enzyme-free cell dissociation buffer (Gibco), centrifuged, and suspended in assay
355 media (DMEM with 0.1% BSA for mammalian cells, unsupplemented SFX-100 insect medium for S2). The
356 aequorin cofactor coelenterazine-F (Nanolight) was added (5 µM final concentration) to the cell
357 suspension, in the dark, with gentle stirring for 2 to 3 hours before assay. For water-insoluble compounds
358 like DEET an emulsion was prepared by adding a percentage of DEET indicated, vol/vol to assay media,
359 vortexed, and bath-sonicated for at least 15 min, but up to one hour. Cells (100 µl, at approx. 50,000 cells)
360 were injected into a 96 well plate containing 100 DEET µl emulsion, and resulting luminescence recorded
361 on a BMG Labtech Lumistar Omega plate reading luminometer. Thapsigargin was added to the cell
362 suspension were indicated to a final concentration of 1 µM, 10 minutes before assay.

363 **Chemical Informatics**

364 ***Machine learning predictions of insect repellency***

365 Physicochemical features for figures 1-2 were selected using Sequential Forward Selection (SFS) (Haddad
366 et al., 2008) from 3,224 using Dragon software (Talete). This algorithm is an iterative search over the
367 chemical feature pool that seeks to maximize the correlation between chemical feature values and, here,
368 the % repellency. These chemical features were subsequently used to fit a support vector machine (SVM)
369 with a radial basis function kernel (RBF). The implementation of the support vector machine algorithm is
370 from the e1071 R package. We performed 20 independent 5-fold cross-validations followed by a receiver
371 operating characteristics (ROC) analysis to analyze the performance of the repellency prediction method.

372 The trained SVM then ranked both a library obtained from eMolecules (http://www.emolecules.com)
373 (>400,000) and natural odor libraries (Supplementary Material) (>3,000) by the repellency score estimates
374 and the set of optimally predictive chemical features. The EPI Suite
375 (http://www.epa.gov/oppt/exposure/pubs/episuite.htm) was used to calculate predicted LogP and Vapor
376 Pressure values.

377 For Figures 3, 5, S1-S2, we updated the methods and algorithms to further optimize the pipeline.
378 Physicochemical features were selected using AlvaDesc software, which offers > 5000 chemical features.
379 Optimal chemical features were then selected using cross-validation and recursive feature elimination
380 algorithm (CV-RFE). The RFE CV algorithm involves iterative partitioning of the data and the selection of
381 feature subsets (n_1, n_2, …, n_{i+1}; where "n" is the size of the feature subset and "i" is an arbitrary indexer).
382 Given a data partition and n features, an arbitrary ML algorithm is fit, importance is assigned to the feature
383 set and the model of n features predicts a test partition, that is, data excluded from training,
384 differentiating the CV-RFE from RFE alone. In this study, the ML algorithm was a support vector machine
385 (SVM) or a random forest. Over 100s of iterations the algorithm converges on the optimal (n) number of
386 features to maximize predictive success. Additionally, for every round the contribution of each chemical
387 feature is assessed, giving rise to an aggregate rank; namely, the frequency at which a feature has been
388 identified as important to the predictive success. Again, distinguishing the standard RFE algorithm from
389 CV-based adaptation. As for computing importance, the random forest algorithm internally tests the
390 contribution of the features. It accomplished this by fitting multiple decision trees on bootstrap samples
391 of the data. Consequently, a percentage of data has been excluded and serves as a test set. By predicting
392 the test set with and without permuting or shuffling the values of a given feature, the algorithm can then
393 assign an importance according to the % increase in error that is observed after permuting the feature.

394 The support vector machine (SVM) algorithm does not natively perform a comparable
395 bootstrapping procedure as random forest and therefore does not generate a test set to assess feature

396 importance. In this case, an external metric must be supplied to assign the importance. Depending on the
397 type of fit, classification or regression, this is a pseudo R^2, based on non-linear regression, or the AUC for
398 the feature and the outcome that is being predicted (e.g., % repellency). For additional details, refer to
399 the documentation provided with caret package in R.

400

401 ***Machine learning predictions of Ca^{2+} mobilization***

402 Due to the smaller number of observations (datapoints or chemicals) we opted for an ensemble
403 method that could take advantage of more of the available data. Random forest fits multiple decision
404 trees on bootstrap samples of the data, thereby reducing the tendency to overfit to one or few chemicals
405 in the dataset. As compared to the SVM, it has two simple parameters (mtry and ntrees) and the tuning
406 grid (or number combinations of these parameters that need to be tested to optimize performance tends
407 to be small). Accordingly, it is an ideal approach when little is known about the activity being predicted.

408 To further reduce overfitting, we identified a small set of physicochemical features on different
409 subsets of the data and then randomly sampled from this pool. By doing so, the features are slightly
410 underfit, which is the better approach, again, when less is known about the activity being predicted.

411 Additionally, we used two different methods and metrics to independently verify that
412 physicochemical features were indeed predictive of the activity. First, a regression-based approached
413 predicting the raw assay activities. Second, a classification-based approach where the top ~40% of the
414 activity distribution was converted into an "Active" label, assessing predictive success by ROC analysis.
415 Finally, we fit classification models that were otherwise identical but trained on shuffled labels. This
416 ensured that the chance level-performances significantly differed.

417 ***Machine learning predictions of odor perceptual qualities***

We used methods that were developed previously and extensively validated for prediction of human odor characters from chemical structures and are described there (Kowalewski et al., 2021; Kowalewski & Ray, 2020b). Briefly, perceptual training data was from a study published in a reference book: ATLAS of Odor Character Profiles (Dravnieks, 1985). In the study, panelists supplied ratings for ~150 odorants and mixtures across 146 possible descriptors; the ratings are reported as the % usage. The % usage refers to the portion of panelists that rated an odorant (1-5) using a particular descriptor (1-146), indicating its relevance to the odorant. It is on the scale 0-100, with the maximum of 100% suggesting every participant found the descriptor to be relevant. The top perceptual descriptors were selected by thresholding the predictions based on the mean value in the training data. For each descriptor in the training data, thresholds were computed as 2x the mean. These thresholds were then applied to the predicted repellents to generate a set of exemplar descriptors. Subsequently, these exemplars were converted into a descriptor frequency table, where the frequency is the total number of occurrences of a descriptor. The data and word cloud plot were generated using the R programming language, with additional functionality provided by the Wordcloud package in R.

RESOURCE AVAILABILITY

Lead Contact

Anandasankar Ray, anand.ray@ucr.edu

Materials Availability

No new materials were generated in this study.

Data and Code Availability

Data used in the analyses is publicly available from the references cited, and the data generated in this manuscript are supplied within the figures. Any additional data associated with this manuscript is also available in other formats on request from the corresponding author and lead contact.

The code developed for this study is available from the corresponding author for non-commercial use upon request. Use of the code may be subject to a standard Material Transfer Agreement (MTA) or specialized licensing agreement through University of California Riverside's Technology Transfer Office, as patent applications related to this software are currently pending.

ACKNOWLEDGMENTS

This work was partially funded by University of California Riverside internal HATCH funding and partially funded by NIDCD and NIAID. The content is solely the responsibility of the authors and does not represent the official views of the funding agencies. The funders had no role in study design, data collection and analysis, decision to publish, or preparation of the manuscript.

AUTHOR CONTRIBUTIONS

J.K., S.M.B., R.A. and A.R. conceived the study. J.K. and S.M.B. planned and executed the computational analysis. R.A. planned and executed the cell line experiments and J.A. performed the insect behavior experiments. J.K. and A.R. wrote the manuscript with contributions from others.

DECLARATION OF INTERESTS

J.K., S.M.B., and A.R. are listed as inventors on various patent applications filed by the university. A.R. is the founder of Sensorygen Inc., that has licensed some of the intellectual property, and A.R. is also the founder of startup companies: Remote Epigenetics, and Sensorygen. Sensorygen has licenses to some of the IP from UCR and is involved in finding new flavors and insect repellents.

464 **REFERENCES**

465 Beglari, M., Goudarzi, N., Shahsavani, D., Arab Chamjangali, M., & Mozafari, Z. (2020). Combination of
466 radial distribution functions as structural descriptors with ligand-receptor interaction information
467 in the QSAR study of some 4-anilinoquinazoline derivatives as potent EGFR inhibitors. *Structural*
468 *Chemistry*, *31*(4), 1481–1491. https://doi.org/10.1007/s11224-020-01505-z

469 Boyle, S. M., McInally, S., & Ray, A. (2013). Expanding the olfactory code by in silico decoding of odor-
470 receptor chemical space. *ELife*, *2013*(2). https://doi.org/10.7554/eLife.01120.001

471 Boyle, S.M., Guda, T., Pham, C.K., Tharadra, S.K., Dahanukar, A., & Ray, A. (2016). Natural DEET
472 substitutes that are strong olfactory repellents of mosquitoes and flies.
473 bioRxiv 060178; doi: https://doi.org/10.1101/060178

474 Briassoulis, G. (2001). Toxic encephalopathy associated with use of DEET insect repellents: A case
475 analysis of its toxicity in children. *Human and Experimental Toxicology*.
476 https://doi.org/10.1191/096032701676731093

477 Buck L and Axel, R. (1991). A Novel Multigene Family May Encode Odorant Receptors: A Molecular Basis.
478 *Cell*, *65*, 175–187.

479 Carey, A. F., Wang, G., Su, C. Y., Zwiebel, L. J., & Carlson, J. R. (2010). Odorant reception in the malaria
480 mosquito Anopheles gambiae. *Nature*. https://doi.org/10.1038/nature08834

481 Cheng, Z., Zhang, Y., & Fu, W. (2010). QSAR study of carboxylic acid derivatives as HIV-1 Integrase
482 inhibitors. *European Journal of Medicinal Chemistry*. https://doi.org/10.1016/j.ejmech.2010.05.052

483 Clem, J. R., Havemann, D. F., & Raebel, M. A. (1993). Insect Repellent (N,N-Diethyl-m-Toluamide)
484 Cardiovascular Toxicity in an Adult. *Annals of Pharmacotherapy*.
485 https://doi.org/10.1177/106002809302700305

Clyne, P. J., Warr, C. G., & Carlson, J. R. (2000). Candidate taste receptors in Drosophila. *Science*. https://doi.org/10.1126/science.287.5459.1830

Clyne, P. J., Warr, C. G., Freeman, M. R., Lessing, D., Kim, J., & Carlson, J. R. (1999). A Novel Family of Divergent Seven-Transmembrane Proteins: Candidate Odorant Receptors in Drosophila. *Neuron*, *22*(2), 327–338. https://doi.org/10.1016/S0896-6273(00)81093-4

Corbel, V., Stankiewicz, M., Pennetier, C., Fournier, D., Stojan, J., Girard, E., Dimitrov, M., Molgó, J., Hougard, J. M., & Lapied, B. (2009). Evidence for inhibition of cholinesterases in insect and mammalian nervous systems by the insect repellent deet. *BMC Biology*. https://doi.org/10.1186/1741-7007-7-47

Deletre, E., Martin, T., Duménil, C., & Chandre, F. (2019). Insecticide resistance modifies mosquito response to DEET and natural repellents. *Parasites & Vectors*, *12*(1), 89. https://doi.org/10.1186/s13071-019-3343-9

Dennis, E. J., Dobosiewicz, M., Jin, X., Duvall, L. B., Hartman, P. S., Bargmann, C. I., & Vosshall, L. B. (2018). A natural variant and engineered mutation in a GPCR promote DEET resistance in C. elegans. *Nature*. https://doi.org/10.1038/s41586-018-0546-8

Devinyak, O., Havrylyuk, D., & Lesyk, R. (2014). 3D-MoRSE descriptors explained. *Journal of Molecular Graphics and Modelling*. https://doi.org/10.1016/j.jmgm.2014.10.006

Dravnieks, A. (1985). *Atlas of Odor Character Profiles*. ASTM. https://doi.org/10.1520/DS61-EB

Duneau, D., Sun, H., Revah, J., San Miguel, K., Kunerth, H. D., Caldas, I. V, Messer, P. W., Scott, J. G., & Buchon, N. (2018). Signatures of Insecticide Selection in the Genome of Drosophila melanogaster. *G3 (Bethesda, Md.)*, *8*(11), 3469–3480. https://doi.org/10.1534/g3.118.200537

González, M. P., Terán, C., Teijeira, M., & Helguera, A. M. (2006). QSAR Studies Using Radial Distribution

Function for Predicting A1 Adenosine Receptors Agonists. *Bulletin of Mathematical Biology*, *69*(1), 347. https://doi.org/10.1007/s11538-006-9127-3

Grabe, V., & Sachse, S. (2018). Fundamental principles of the olfactory code. In *BioSystems*. https://doi.org/10.1016/j.biosystems.2017.10.010

Grant, G. G., & Hall, A. C. (2019). Interactions of N, N- diethyl-meta-toluamide (DEET) and Novel Insect Repellents with Mammalian GABAA and Glycine Receptors. *The FASEB Journal*, *33*(1_supplement), 813.13-813.13. https://doi.org/10.1096/fasebj.2019.33.1_supplement.813.13

Gupta, R. K., & Bhattacharjee, A. (2006). *Discovery and Design of New Arthropod/Insect Repellents by Computer-Aided Molecular Modeling* (pp. 195 – 228). https://doi.org/10.1201/9781420006650.ch10

Haddad, R., Khan, R., Takahashi, Y. K., Mori, K., Harel, D., & Sobel, N. (2008). A metric for odorant comparison. *Nature Methods*. https://doi.org/10.1038/nmeth.1197

Hallem, E. A., & Carlson, J. R. (2006). Coding of Odors by a Receptor Repertoire. *Cell*, *125*(1), 143–160. https://doi.org/http://dx.doi.org/10.1016/j.cell.2006.01.050

Hemmer, M. C., Steinhauer, V., & Gasteiger, J. (1999). Deriving the 3D structure of organic molecules from their infrared spectra. *Vibrational Spectroscopy*. https://doi.org/10.1016/s0924-2031(99)00014-4

Katritzky, A. R., Wang, Z., Slavov, S., Tsikolia, M., Dobchev, D., Akhmedov, N. G., Hall, C. D., Bernier, U. R., Clark, G. G., & Linthicum, K. J. (2008). Synthesis and bioassay of improved mosquito repellents predicted from chemical structure. *Proceedings of the National Academy of Sciences of the United States of America*. https://doi.org/10.1073/pnas.0800571105

Keller, A., Gerkin, R. C., Guan, Y., Dhurandhar, A., Turu, G., Szalai, B., Mainland, J. D., Ihara, Y., Yu, C. W.,

Wolfinger, R., Vens, C., Schietgat, L., De Grave, K., Norel, R., Stolovitzky, G., Cecchi, G. A., Vosshall, L. B., & Meyer, P. (2017). Predicting human olfactory perception from chemical features of odor molecules. *Science*, *355*(6327), 820–826. https://doi.org/10.1126/science.aal2014

Kleinau, G., Pratzka, J., Nürnberg, D., Grüters, A., Führer-Sakel, D., Krude, H., Köhrle, J., Schöneberg, T., & Biebermann, H. (2011). Differential modulation of beta-adrenergic receptor signaling by trace amine-associated receptor 1 agonists. *PLoS ONE*. https://doi.org/10.1371/journal.pone.0027073

Kline, D. L., Bernier, U. R., Posey, K. H., & Barnard, D. R. (2003). Olfactometric Evaluation of Spatial Repellents for Aedes aegypti . *Journal of Medical Entomology*. https://doi.org/10.1603/0022-2585-40.4.463

Klocke, J. A., Darlington, M. V., & Balandrin, M. F. (1987). 1,8-Cineole (Eucalyptol), a mosquito feeding and ovipositional repellent from volatile oil of Hemizonia fitchii (Asteraceae). *Journal of Chemical Ecology*. https://doi.org/10.1007/BF01012562

Kowalewski, J., Huynh, B., & Ray, A. (2021). A systems-wide understanding of the human olfactory percept chemical space. *Chemical Senses*. https://doi.org/10.1093/chemse/bjab007

Kowalewski, J., & Ray, A. (2020a). Predicting novel drugs for SARS-CoV-2 using machine learning from a >10 million chemical space. *Heliyon*. https://doi.org/10.1016/j.heliyon.2020.e04639

Kowalewski, J., & Ray, A. (2020b). Predicting Human Olfactory Perception from Activities of Odorant Receptors. *IScience*, *23*(8), 101361. https://doi.org/10.1016/j.isci.2020.101361

Lee, B. K., Mayhew, E. J., Sanchez-Lengelin, B., Wei, J. N., Qian, W. W., Little, K. A., Andres, M. A., Nguyen, B. B., Moloy, T., Yasonik, J., Parker, J. K., Gerkin, R. C., Mainland, J. D., & Wiltschko, A. B. (2023). A principal odor map unifies diverse tasks in olfactory perception. *Science*. https://doi.org/10.1126/science.ade4401

MacWilliam, D., Kowalewski, J., Kumar, A., Pontrello, C., & Ray, A. (2018). Signaling Mode of the Broad-Spectrum Conserved CO2 Receptor Is One of the Important Determinants of Odor Valence in Drosophila. *Neuron*. https://doi.org/10.1016/j.neuron.2018.01.028

Maldonado, A. G., Doucet, J. P., Petitjean, M., & Fan, B. T. (2006). Molecular similarity and diversity in chemoinformatics: From theory to applications. In *Molecular Diversity*. https://doi.org/10.1007/s11030-006-8697-1

Mombaerts, P. (1999). Molecular biology of odorant receptors in vertebrates. *Annual Review of Neuroscience*, *22*, 487–509. https://doi.org/10.1146/annurev.neuro.22.1.487

Mombaerts, Peter. (2001). THE HUMAN REPERTOIRE OF ODORANT RECEPTOR GENES AND PSEUDOGENES. *Annual Review of Genomics and Human Genetics*, *2*(1), 493–510. https://doi.org/10.1146/annurev.genom.2.1.493

Osimitz, T. G., Murphy, J. V., Fell, L. A., & Page, B. (2010). Adverse events associated with the use of insect repellents containing N,N-diethyl-m-toluamide (DEET). *Regulatory Toxicology and Pharmacology*. https://doi.org/10.1016/j.yrtph.2009.09.004

Reeder, N. L., Ganz, P. J., Carlson, J. R., & Saunders, C. W. (2009). Isolation of a Deet-Insensitive Mutant of <I>Drosophila melanogaster</I> (Diptera: Drosophilidae). *Journal of Economic Entomology*. https://doi.org/10.1603/0022-0493-94.6.1584

Sachse, S., & Beshel, J. (2016). The good, the bad, and the hungry: How the central brain codes odor valence to facilitate food approach in Drosophila. In *Current Opinion in Neurobiology*. https://doi.org/10.1016/j.conb.2016.06.012

Sanchez-Lengeling, B., Wei, J. N., Lee, B. K., Gerkin, R. C., Aspuru-Guzik, A., & Wiltschko, A. B. (2019). *Machine Learning for Scent: Learning Generalizable Perceptual Representations of Small Molecules*.

https://arxiv.org/abs/1910.10685

Schoenig, G. P., Hartnagel, R. E., Osimitz, T. G., & Llanso, S. (1996). Absorption, distribution, metabolism, and excretion of N,N-diethyl-M-toluamide in the rat. *Drug Metabolism and Disposition*.

Selim, S., Hartnagel, R. E., Osimitz, T. G., Gabriel, K. L., & Schoenig, G. P. (1995). Absorption, metabolism, and excretion of N,N-diethyl-m-toluamide following dermal application to human volunteers. *Toxicological Sciences*. https://doi.org/10.1093/toxsci/25.1.95

Swale, D. R., Sun, B., Tong, F., & Bloomquist, J. R. (2014). Neurotoxicity and mode of action of N, N-diethyl-Meta-toluamide (DEET). *PLoS ONE*. https://doi.org/10.1371/journal.pone.0103713

Syed, Z., & Leal, W. S. (2008). Mosquitoes smell and avoid the insect repellent DEET. *Proceedings of the National Academy of Sciences of the United States of America*. https://doi.org/10.1073/pnas.0805312105

Syed, Z., Pelletier, J., Flounders, E., Chitolina, R. F., & Leal, W. S. (2011). Generic insect repellent detector from the fruit fly Drosophila melanogaster. *PLoS ONE*. https://doi.org/10.1371/journal.pone.0017705

Tavares, E. M., Judge, B. S., & Jones, J. S. (2019). Bug off! Severe toxicity following inhalational exposure to N, N-diethyl-meta-toluamide (DEET). *American Journal of Emergency Medicine*. https://doi.org/10.1016/j.ajem.2019.04.019

Vassar, R., Ngai, J., & Axel, R. (1993). Spatial segregation of odorant receptor expression in the mammalian olfactory epithelium. *Cell*, *74*(2), 309–318. https://doi.org/0092-8674(93)90422-M [pii]

595 **FIGURE LEGENDS**

596 **Figure 1. A chemical informatics pipeline to screen for pleasant smelling insect repellents**

597 **A**, Overview of the cheminformatics pipeline used to identify novel DEET-like ligands from a larger
598 chemical space. Summary table of top 10 physicochemical features that optimally corelate with
599 repellency. Receiver-operating-characteristic curve (ROC), which indicates the success in predicting test
600 repellents. The performance is the average over 100 80/20 splits, where 80% of the data is for training
601 and 20% for testing. The mean area under the curve (AUC) is provided. Representative structures from
602 the top 150 predicted repellent compounds.

603 **Figure 2. Models successfully predict odor perceptual qualities of repellents in humans**

604 **A,** Validation of models predicting the odor perceptual qualities (146 perceptual descriptors) of a set of
605 compounds that were screened for repellency in Figure 3A. The performance metric for the validation is
606 the area under the ROC curve, which assesses the rate of correctly predicted perceptual descriptors
607 relative the rate of incorrectly predicted descriptors. Dashed line is the average Area Under the Curve
608 (AUC). **B,** Sample ROC curves for select compounds as well as the ROC curve across all compounds (e.g.,
609 shown as separate curves in the ROC plot as well as those not shown but whose identities appear in Figure
610 2A); the respective AUC values are reported inside the plot. **C,** The top 25 perceptual descriptors for the
611 predicted repellents that underwent experimental validation are displayed as a word cloud. The font size
612 of the descriptor is scaled relative to frequency.

613 **Figure 3. Experimental validation of predicted insect repellents show a high success rate several of**
614 **which are pleasant smelling**

615 **A,** Representative still photograph of landing assay of female *Aedes aegypti* mosquitoes on filter paper
616 covered heat block over 5 mins (overlay of all frames), and **B,** mean Repellency Coefficient for each of the

617 indicated compounds (by CAS numbers) tested at ~0.2mg/cm^2, N=2-4 trials for each, ~20 mosquitoes/trial.
618 For DEET, N=23 trials. CAS numbers ending in a ".1" are compounds tested at a second lower amount of
619 ~0.06mg/cm^2.

620 **C,** Mean Preference index of *Drosophila* adults to repellents at three different concentrations dissolved in
621 acetone in a Two-choice trap assay baited with 10% Apple Cider Vinegar measured after 48 hrs. N = 7-10
622 trials each treatment at 48 hrs, 10 flies/trial, error bars = s.e.m.

623 **Figure 4. Some, but not all insect repellents increase Ca^{2+} mobilization in a human cell line**

624 DEET induces a non-specific calcium response *in vitro*. **A.** Dose response curves for three mammalian cell
625 lines (HEK293. CHOK1, NG108) and one insect cell line (S2). EC50 and Hill coefficients for each cell line are
626 given below. **B.** Representative DEET induced calcium kinetics in HEK293 cells. **C.** HEK293 cells treated
627 with thapsigargin 10 min before assay to deplete intracellular calcium stores no longer respond to DEET,
628 suggesting DEET response is dependent on intracellular calcium. Error bars are standard deviation. **D. F,**
629 Luminescence of the Ca^{2+} indicator at two different concentrations for predicted and previously known
630 repellent chemicals, scaled relative to DEET.

631 **Figure 5. Screen of 10+ million chemicals predicts several insect repellents with different smells**

632 **A,** Tabulated predicted % repellency (relative to DEET) from a library of 10+ million chemicals, filtered to
633 the top values. The best matching known repellent is displayed alongside the Euclidean distance, the
634 predicted LD50 and Ca^{2+} mobilization. **B**, heatmap organizing top predictions according to estimated
635 perceptual qualities.

636

637

638

639 **Supplemental Figure S1**

640 **A**, Overview of the approach to generate and validate the machine learning models. Here, a model-
641 averaged prediction is made, where each model has access to different physicochemical features and is
642 trained on different combinations of training set chemicals. **B,** The R^2 values over the 100 train/test splits,
643 averaged into 10 bins. **C,** The average classification success is reported over 100 train/test splits, assessed
644 by the area under the ROC curve. Active labels (positive cases) were assigned as chemical scoring in the
645 top ~40% of Ca^{2+} values. This is compared to shuffling the labels before training, reported as "Shuffle."

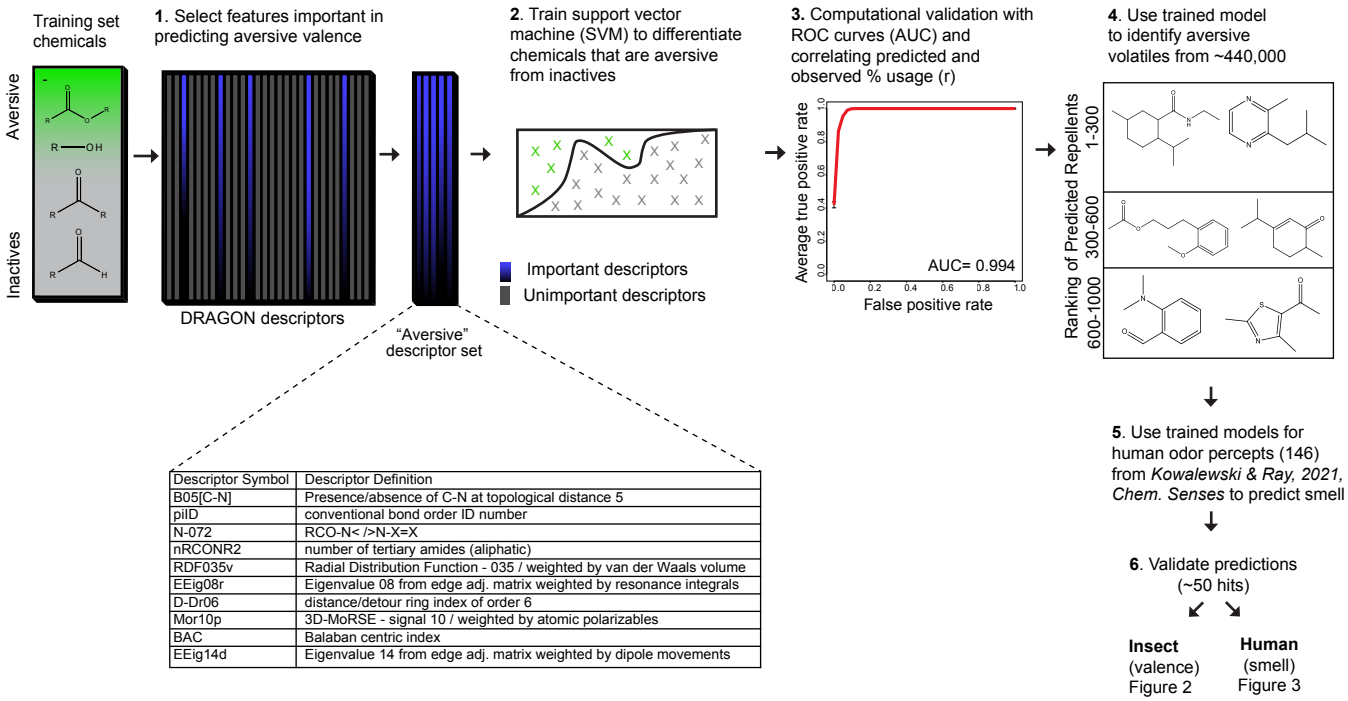

Descriptor Symbol	Descriptor Definition
B05[C-N]	Presence/absence of C-N at topological distance 5
piID	conventional bond order ID number
N-072	RCO-N< />N-X=X
nRCONR2	number of tertiary amides (aliphatic)
RDF035v	Radial Distribution Function - 035 / weighted by van der Waals volume
EEig08r	Eigenvalue 08 from edge adj. matrix weighted by resonance integrals
D-Dr06	distance/detour ring index of order 6
Mor10p	3D-MoRSE - signal 10 / weighted by atomic polarizables
BAC	Balaban centric index
EEig14d	Eigenvalue 14 from edge adj. matrix weighted by dipole movements

Figure 1

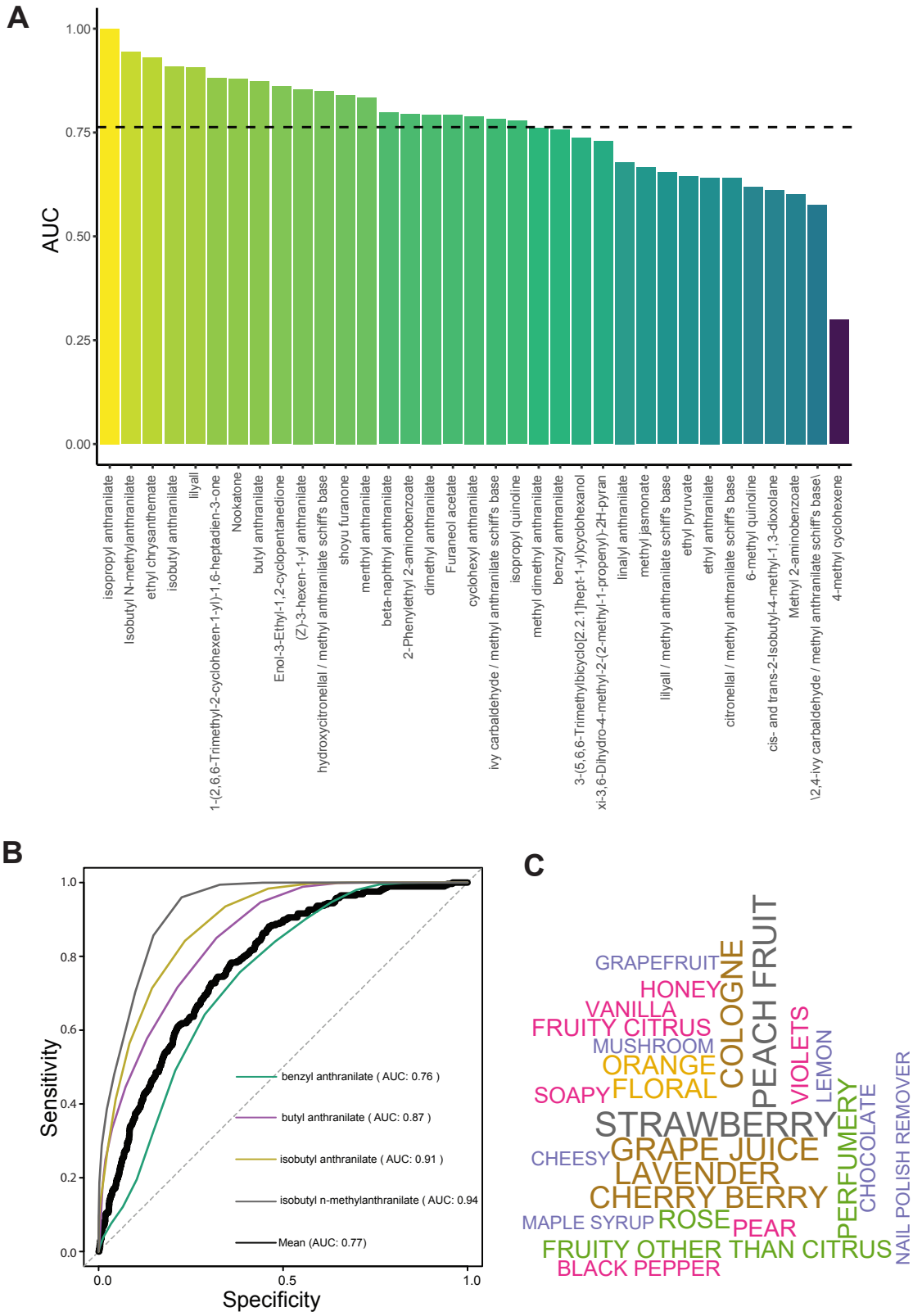
A
AUC
1.00
0.75
0.50
0.25
0.00
isopropyl anthranilate
Isobutyl N-methylanthranilate
ethyl chrysanthemate
isobutyl anthranilate
lilyall
1-(2,6,6-Trimethyl-2-cyclohexen-1-yl)-1,6-heptadien-3-one
Nookatone
butyl anthranilate
Enol-3-Ethyl-1,2-cyclopentanedione
(Z)-3-hexen-1-yl anthranilate
hydroxycitronellal / methyl anthranilate schiff's base
shoyu furanone
menthyl anthranilate
beta-naphthyl anthranilate
2-Phenylethyl 2-aminobenzoate
dimethyl anthranilate
Furaneol acetate
cyclohexyl anthranilate
ivy carbaldehyde / methyl anthranilate schiff's base
isopropyl quinoline
methyl dimethyl anthranilate
benzyl anthranilate
3-(5,6,6-Trimethylbicyclo[2.2.1]hept-1-yl)cyclohexanol
xi-3,6-Dihydro-4-methyl-2-(2-methyl-1-propenyl)-2H-pyran
linalyl anthranilate
methyl jasmonate
lilyall / methyl anthranilate schiff's base
ethyl pyruvate
ethyl anthranilate
citronellal / methyl anthranilate schiff's base
6-methyl quinoline
cis- and trans-2-Isobutyl-4-methyl-1,3-dioxolane
Methyl 2-aminobenzoate
\2,4-ivy carbaldehyde / methyl anthranilate schiff's base\
4-methyl cyclohexene
B
Sensitivity
Specificity
1.0
0.8
0.6
0.4
0.2
0.0
0.0
0.5
1.0
benzyl anthranilate (AUC: 0.76)
butyl anthranilate (AUC: 0.87)
isobutyl anthranilate (AUC: 0.91)
isobutyl n-methylanthranilate (AUC: 0.94
Mean (AUC: 0.77)
C
GRAPEFRUIT
HONEY
VANILLA
FRUITY CITRUS
MUSHROOM
ORANGE
SOAPY
FLORAL
COLOGNE
PEACH
FRUIT
VIOLETS
LEMON
STRAWBERRY
CHEESY
GRAPE JUICE
LAVENDER
CHERRY BERRY
MAPLE SYRUP
ROSE
PEAR
PERFUMERY
CHOCOLATE
NAIL POLISH REMOVER
FRUITY OTHER THAN CITRUS
BLACK PEPPER

Figure 2

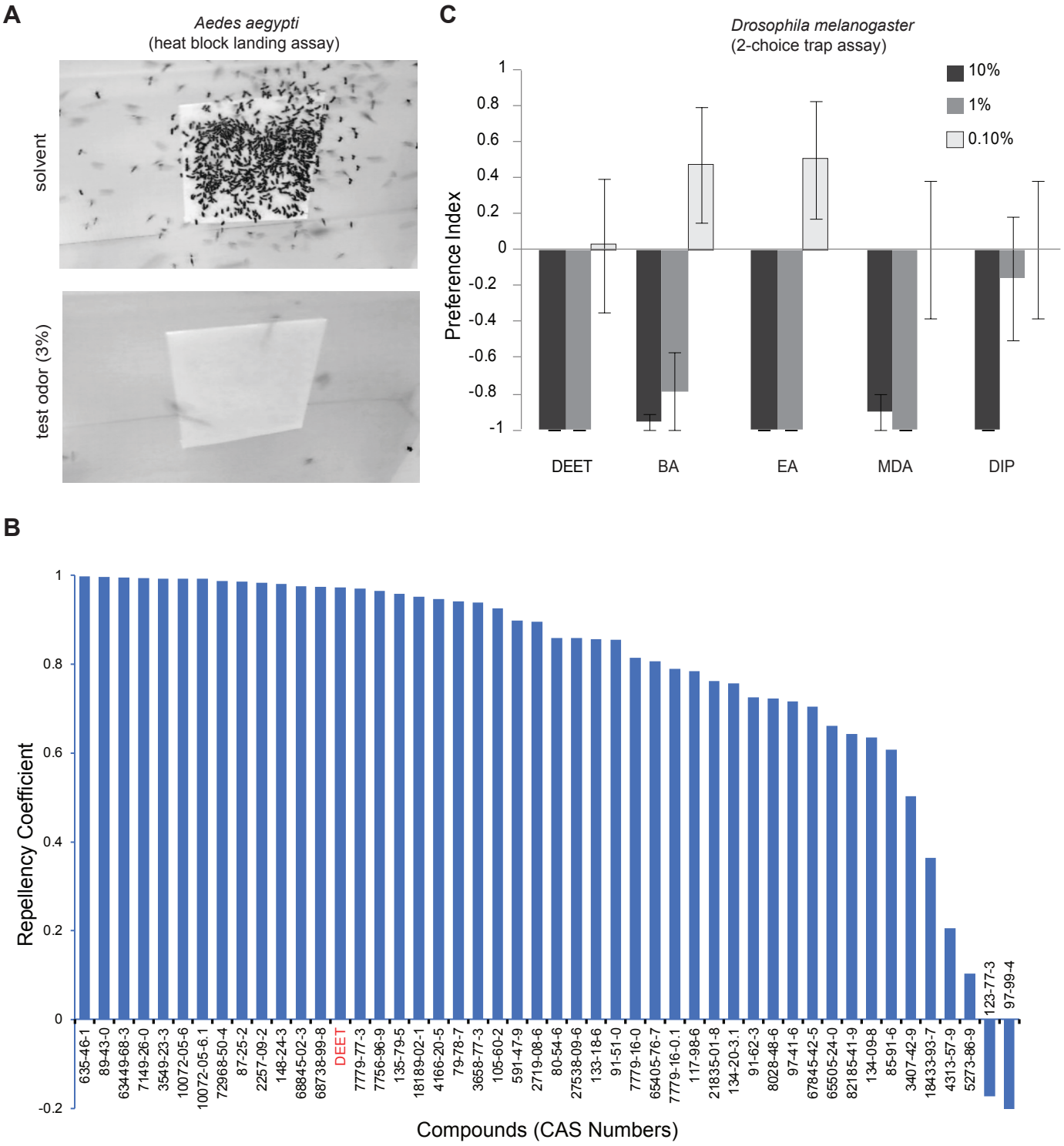
A
Aedes aegypti
(heat block landing assay)
solvent
test odor (3%)
C
Drosophila melanogaster
(2-choice trap assay)
10%
1%
0.10%
Preference Index
1
0.8
0.6
0.4
0.2
0
-0.2
-0.4
-0.6
-0.8
-1
DEET
BA
EA
MDA
DIP
B
Repellency Coefficient
1
0.8
0.6
0.4
0.2
0
-0.2
635-46-1
89-43-0
63449-68-3
7149-26-0
3549-23-3
10072-05-6
10072-05-6.1
72968-50-4
87-25-2
2257-09-2
148-24-3
68845-02-3
68738-99-8
DEET
7779-77-3
7756-96-9
135-79-5
18189-02-1
4166-20-5
79-78-7
3658-77-3
105-60-2
591-47-9
2719-08-6
80-54-6
27538-09-6
133-18-6
91-51-0
7779-16-0
65405-76-7
7779-16-0.1
117-98-6
21835-01-8
134-20-3.1
91-62-3
8028-48-6
97-41-6
67845-42-5
65505-24-0
82185-41-9
134-09-8
85-91-6
3407-42-9
18433-93-7
4313-57-9
5273-86-9
123-77-3
97-99-4
Compounds (CAS Numbers)

Figure 3

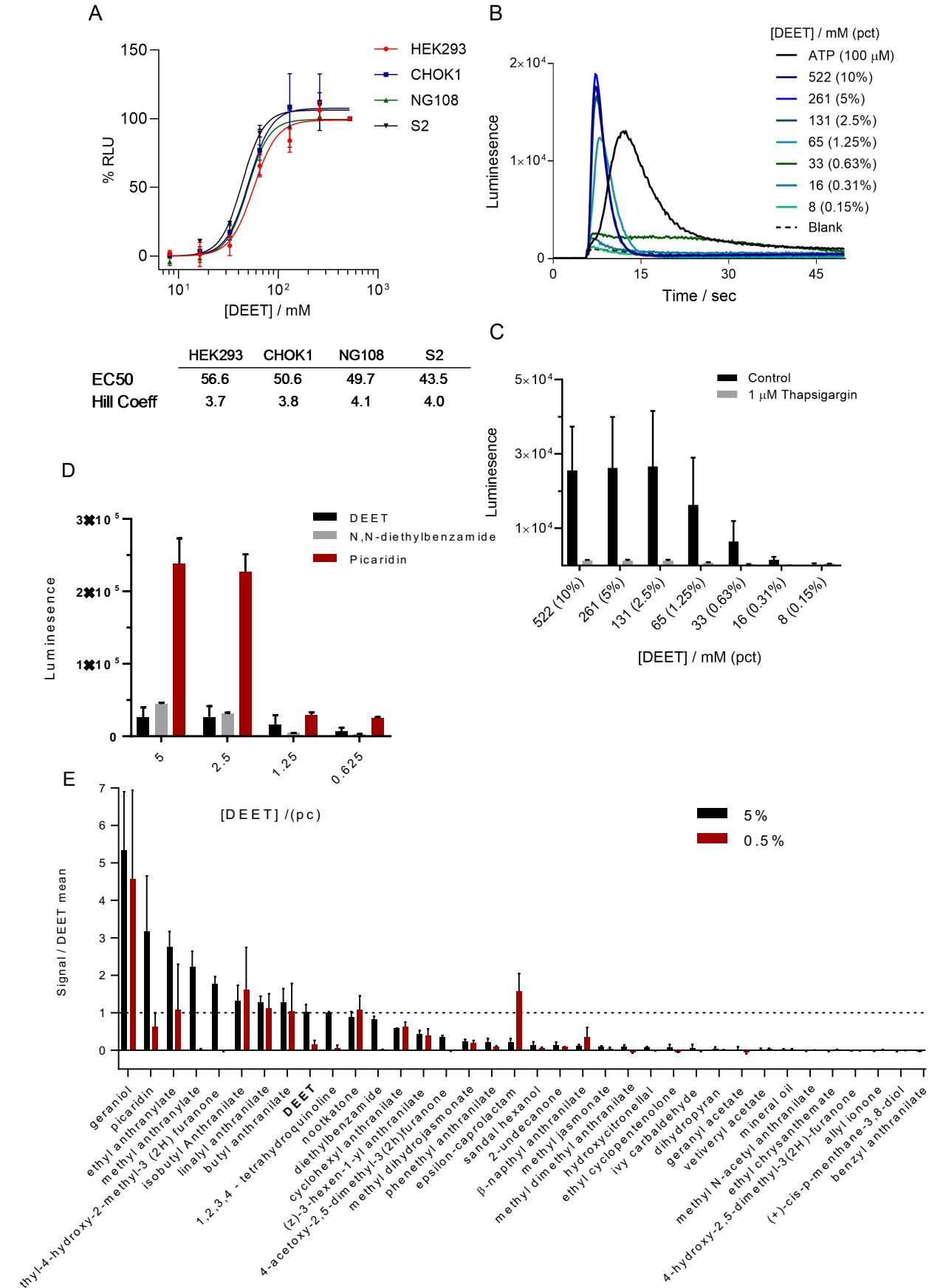

	HEK293	CHOK1	NG108	S2
EC50	56.6	50.6	49.7	43.5
Hill Coeff	3.7	3.8	4.1	4.0

Figure 4

A

Image	ZINC_ID	Score	LD_{50} mg/kg	Ca^{2+} mobilization
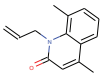	ZINC000001394030	110.9316	1293.0062	0.9054749
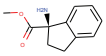	ZINC000034195873	110.5746	711.4268	0.7932151
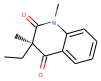	ZINC000005327991	110.4276	883.9981	0.7673523
	ZINC000094992683	110.4188	1067.0473	0.9159867
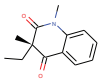	ZINC000001735256	110.4169	883.8132	0.7749915

Image	ZINC_ID	Score	LD_{50} mg/kg	Ca^{2+} mobilization
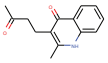	ZINC000008609700	110.2547	1287.3842	0.5077889
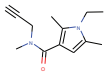	ZINC000253417706	109.7302	933.5598	0.8336481
	ZINC000034195871	109.6462	684.8090	0.9535496
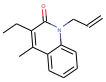	ZINC000000506855	109.5113	1299.5812	0.7571195
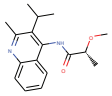	ZINC000191321911	109.5082	989.3195	1.1121364

B

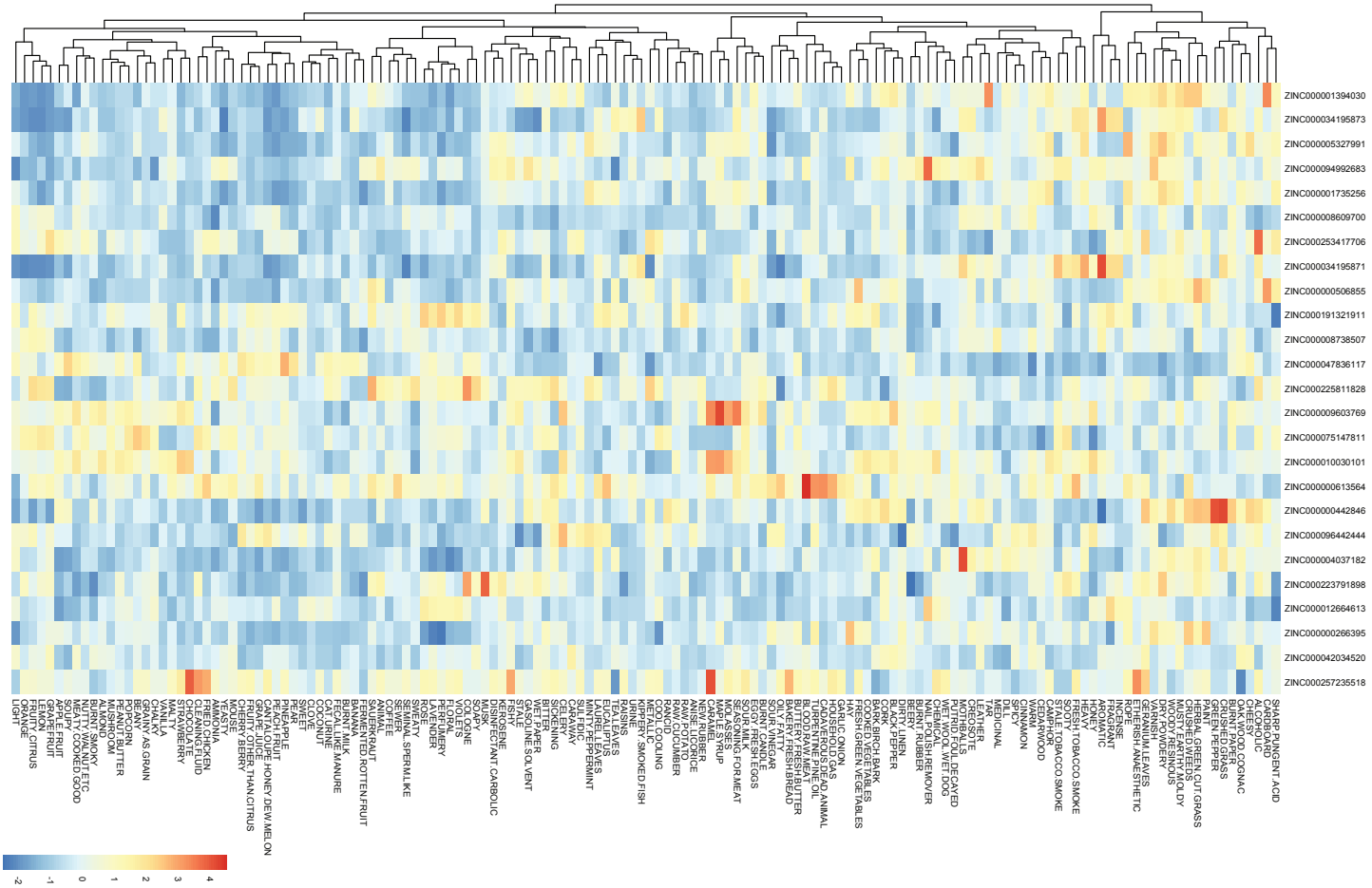

Figure 5